

Dense-Medium Modifications to Jet-Induced Hadron Pair Distributions in Au + Au Collisions at $\sqrt{s_{NN}} = 200$ GeV

S. S. Adler,⁵ S. Afanasiev,¹⁷ C. Aidala,⁵ N. N. Ajitanand,⁴³ Y. Akiba,^{20,38} J. Alexander,⁴³ R. Amirikas,¹² L. Aphecetche,⁴⁵ S. H. Aronson,⁵ R. Averbeck,⁴⁴ T. C. Awes,³⁵ R. Azmoun,⁴⁴ V. Babintsev,¹⁵ A. Baldisseri,¹⁰ K. N. Barish,⁶ P. D. Barnes,²⁷ B. Bassalleck,³³ S. Bathe,³⁰ S. Batsouli,⁹ V. Baublis,³⁷ A. Bazilevsky,^{39,15} S. Belikov,^{16,15} Y. Berdnikov,⁴⁰ S. Bhagavatula,¹⁶ J. G. Boissevain,²⁷ H. Borel,¹⁰ S. Borenstein,²⁵ M. L. Brooks,²⁷ D. S. Brown,³⁴ N. Bruner,³³ D. Bucher,³⁰ H. Buesching,³⁰ V. Bumazhnov,¹⁵ G. Bunce,^{5,39} J. M. Burward-Hoy,^{26,44} S. Butsyk,⁴⁴ X. Camard,⁴⁵ J.-S. Chai,¹⁸ P. Chand,⁴ W. C. Chang,² S. Chernichenko,¹⁵ C. Y. Chi,⁹ J. Chiba,²⁰ M. Chiu,⁹ I. J. Choi,⁵² J. Choi,¹⁹ R. K. Choudhury,⁴ T. Chujo,⁵ V. Ciencialo,³⁵ Y. Cobigo,¹⁰ B. A. Cole,⁹ P. Constantin,¹⁶ D. d'Enterria,⁴⁵ G. David,⁵ H. Delagrange,⁴⁵ A. Denisov,¹⁵ A. Deshpande,³⁹ E. J. Desmond,⁵ A. Devismes,⁴⁴ O. Dietzsch,⁴¹ O. Drapier,²⁵ A. Drees,⁴⁴ R. du Rietz,²⁹ A. Durum,¹⁵ D. Dutta,⁴ Y. V. Efremenko,³⁵ K. El Chenawi,⁴⁹ A. Enokizono,¹⁴ H. En'yo,^{38,39} S. Esumi,⁴⁸ L. Ewell,⁵ D. E. Fields,^{33,39} F. Fleuret,²⁵ S. L. Fokin,²³ B. D. Fox,³⁹ Z. Fraenkel,⁵¹ J. E. Frantz,⁹ A. Franz,⁵ A. D. Frawley,¹² S.-Y. Fung,⁶ S. Garpman,^{29,*} T. K. Ghosh,⁴⁹ A. Glenn,⁴⁶ G. Gogiberidze,⁴⁶ M. Gonin,²⁵ J. Gosset,¹⁰ Y. Goto,³⁹ R. Granier de Cassagnac,²⁵ N. Grau,¹⁶ S. V. Greene,⁴⁹ M. Grosse Perdekamp,³⁹ W. Guryn,⁵ H.-Å. Gustafsson,²⁹ T. Hachiya,¹⁴ J. S. Haggerty,⁵ H. Hamagaki,⁸ A. G. Hansen,²⁷ E. P. Hartouni,²⁶ M. Harvey,⁵ R. Hayano,⁸ N. Hayashi,³⁸ X. He,¹³ M. Heffner,²⁶ T. K. Hemmick,⁴⁴ J. M. Heuser,⁴⁴ M. Hibino,⁵⁰ J. C. Hill,¹⁶ W. Holzmann,⁴³ K. Homma,¹⁴ B. Hong,²² A. Hoover,³⁴ T. Ichihara,^{38,39} V. V. Ikonnikov,²³ K. Imai,^{24,38} D. Isenhower,¹ M. Ishihara,³⁸ M. Issah,⁴³ A. Isupov,¹⁷ B. V. Jacak,⁴⁴ W. Y. Jang,²² Y. Jeong,¹⁹ J. Jia,⁴⁴ O. Jinnouchi,³⁸ B. M. Johnson,⁵ S. C. Johnson,²⁶ K. S. Joo,³¹ D. Jouan,³⁶ S. Kametani,^{8,50} N. Kamihara,^{47,38} J. H. Kang,⁵² S. S. Kapoor,⁴ K. Katou,⁵⁰ S. Kelly,⁹ B. Khachaturov,⁵¹ A. Khanzadeev,³⁷ J. Kikuchi,⁵⁰ D. H. Kim,³¹ D. J. Kim,⁵² D. W. Kim,¹⁹ E. Kim,⁴² G.-B. Kim,²⁵ H. J. Kim,⁵² E. Kistenev,⁵ A. Kiyomichi,⁴⁸ K. Kiyoyama,³² C. Klein-Boesing,³⁰ H. Kobayashi,^{38,39} L. Kochenda,³⁷ V. Kochetkov,¹⁵ D. Koehler,³³ T. Kohama,¹⁴ M. Kopytine,⁴⁴ D. Kotchetkov,⁶ A. Kozlov,⁵¹ P. J. Kroon,⁵ C. H. Kuberg,^{1,27,*} K. Kurita,³⁹ Y. Kuroki,⁴⁸ M. J. Kweon,²² Y. Kwon,⁵² G. S. Kyle,³⁴ R. Lacey,⁴³ V. Ladygin,¹⁷ J. G. Lajoie,¹⁶ A. Lebedev,^{16,23} S. Leckey,⁴⁴ D. M. Lee,²⁷ S. Lee,¹⁹ M. J. Leitch,²⁷ X. H. Li,⁶ H. Lim,⁴² A. Litvinenko,¹⁷ M. X. Liu,²⁷ Y. Liu,³⁶ C. F. Maguire,⁴⁹ Y. I. Makdisi,⁵ A. Malakhov,¹⁷ V. I. Manko,²³ Y. Mao,^{7,38} G. Martinez,⁴⁵ M. D. Marx,⁴⁴ H. Masui,⁴⁸ F. Matathias,⁴⁴ T. Matsumoto,^{8,50} P. L. McGaughey,²⁷ E. Melnikov,¹⁵ F. Messer,⁴⁴ Y. Miake,⁴⁸ J. Milan,⁴³ T. E. Miller,⁴⁹ A. Milov,^{44,51} S. Mioduszewski,⁵ R. E. Mischke,²⁷ G. C. Mishra,¹³ J. T. Mitchell,⁵ A. K. Mohanty,⁴ D. P. Morrison,⁵ J. M. Moss,²⁷ F. Mühlbacher,⁴⁴ D. Mukhopadhyay,⁵¹ M. Muniruzzaman,⁶ J. Murata,^{38,39} S. Nagamiya,²⁰ J. L. Nagle,⁹ T. Nakamura,¹⁴ B. K. Nandi,⁶ M. Nara,⁴⁸ J. Newby,⁴⁶ P. Nilsson,²⁹ A. S. Nyanin,²³ J. Nystrand,²⁹ E. O'Brien,⁵ C. A. Ogilvie,¹⁶ H. Ohnishi,^{5,38} I. D. Ojha,^{49,3} K. Okada,³⁸ M. Ono,⁴⁸ V. Onuchin,¹⁵ A. Oskarsson,²⁹ I. Otterlund,²⁹ K. Oyama,⁸ K. Ozawa,⁸ D. Pal,⁵¹ A. P. T. Palounek,²⁷ V. Pantuev,⁴⁴ V. Papavassiliou,³⁴ J. Park,⁴² A. Parmar,³³ S. F. Pate,³⁴ T. Peitzmann,³⁰ J.-C. Peng,²⁷ V. Peresedov,¹⁷ C. Pinkenburg,⁵ R. P. Pisani,⁵ F. Plasil,³⁵ M. L. Purschke,⁵ A. K. Purwar,⁴⁴ J. Rak,¹⁶ I. Ravinovich,⁵¹ K. F. Read,^{35,46} M. Reuter,⁴⁴ K. Reygers,³⁰ V. Riabov,^{37,40} Y. Riabov,³⁷ G. Roche,²⁸ A. Romana,^{25,*} M. Rosati,¹⁶ P. Rosnet,²⁸ S. S. Ryu,⁵² M. E. Sadler,¹ N. Saito,^{38,39} T. Sakaguchi,^{8,50} M. Sakai,³² S. Sakai,⁴⁸ V. Samsonov,³⁷ L. Sanfratello,³³ R. Santo,³⁰ H. D. Sato,^{24,38} S. Sato,^{5,48} S. Sawada,²⁰ Y. Schutz,⁴⁵ V. Semenov,¹⁵ R. Seto,⁶ M. R. Shaw,^{1,27} T. K. Shea,⁵ T.-A. Shibata,^{47,38} K. Shigaki,^{14,20} T. Shiina,²⁷ C. L. Silva,⁴¹ D. Silvermyr,^{27,29} K. S. Sim,²² C. P. Singh,³ V. Singh,³ M. Sivertz,⁵ A. Soldatov,¹⁵ R. A. Soltz,²⁶ W. E. Sondheim,²⁷ S. P. Sorensen,⁴⁶ I. V. Sourikova,⁵ F. Staley,¹⁰ P. W. Stankus,³⁵ E. Stenlund,²⁹ M. Stepanov,³⁴ A. Ster,²¹ S. P. Stoll,⁵ T. Sugitate,¹⁴ J. P. Sullivan,²⁷ E. M. Takagui,⁴¹ A. Taketani,^{38,39} M. Tamai,⁵⁰ K. H. Tanaka,²⁰ Y. Tanaka,³² K. Tanida,³⁸ M. J. Tannenbaum,⁵ P. Tarján,¹¹ J. D. Tepe,^{1,27} T. L. Thomas,³³ J. Tojo,^{24,38} H. Torii,^{24,38} R. S. Towell,¹ I. Tserruya,⁵¹ H. Tsuruoka,⁴⁸ S. K. Tuli,³ H. Tydesjö,²⁹ N. Tyurin,¹⁵ H. W. van Hecke,²⁷ J. Velkovska,^{5,44} M. Velkovsky,⁴⁴ V. Veszprémi,¹¹ L. Villatte,⁴⁶ A. A. Vinogradov,²³ M. A. Volkov,²³ E. Vznuzdaev,³⁷ X. R. Wang,¹³ Y. Watanabe,^{38,39} S. N. White,⁵ F. K. Wohn,¹⁶ C. L. Woody,⁵ W. Xie,⁶ Y. Yang,⁷ A. Yanovich,¹⁵ S. Yokkaichi,^{38,39} G. R. Young,³⁵ I. E. Yushmanov,²³ W. A. Zajc,^{9,†} C. Zhang,⁹ S. Zhou,⁷ S. J. Zhou,⁵¹ and L. Zolin¹⁷

(PHENIX Collaboration)

¹Abilene Christian University, Abilene, Texas 79699, USA

²Institute of Physics, Academia Sinica, Taipei 11529, Taiwan

³Department of Physics, Banaras Hindu University, Varanasi 221005, India

- ⁴Bhabha Atomic Research Centre, Bombay 400 085, India
⁵Brookhaven National Laboratory, Upton, New York 11973-5000, USA
⁶University of California—Riverside, Riverside, California 92521, USA
⁷China Institute of Atomic Energy (CIAE), Beijing, People's Republic of China
⁸Center for Nuclear Study, Graduate School of Science, University of Tokyo, 7-3-1 Hongo, Bunkyo, Tokyo 113-0033, Japan
⁹Columbia University, New York, New York 10027, USA,
and Nevis Laboratories, Irvington, New York 10533, USA
¹⁰Dapnia, CEA Saclay, F-91191 Gif-sur-Yvette, France
¹¹Debrecen University, H-4010 Debrecen, Egyetem tér 1, Hungary
¹²Florida State University, Tallahassee, Florida 32306, USA
¹³Georgia State University, Atlanta, Georgia 30303, USA
¹⁴Hiroshima University, Kagamiyama, Higashi-Hiroshima 739-8526, Japan
¹⁵IHEP Protvino, State Research Center of Russian Federation, Institute for High Energy Physics, Protvino 142281, Russia
¹⁶Iowa State University, Ames, Iowa 50011, USA
¹⁷Joint Institute for Nuclear Research, 141980 Dubna, Moscow Region, Russia
¹⁸KAERI, Cyclotron Application Laboratory, Seoul, South Korea
¹⁹Kangnung National University, Kangnung 210-702, South Korea
²⁰KEK, High Energy Accelerator Research Organization, Tsukuba, Ibaraki 305-0801, Japan
²¹KFKI Research Institute for Particle and Nuclear Physics of the Hungarian Academy of Sciences (MTA KFKI RMKI),
H-1525 Budapest 114, P.O. Box 49, Budapest, Hungary
²²Korea University, Seoul 136-701, Korea
²³Russian Research Center "Kurchatov Institute," Moscow, Russia
²⁴Kyoto University, Kyoto 606-8502, Japan
²⁵Laboratoire Leprince-Ringuet, Ecole Polytechnique, CNRS-IN2P3, Route de Saclay, F-91128 Palaiseau, France
²⁶Lawrence Livermore National Laboratory, Livermore, California 94550, USA
²⁷Los Alamos National Laboratory, Los Alamos, New Mexico 87545, USA
²⁸LPC, Université Blaise Pascal, CNRS-IN2P3, Clermont-Fd, 63177 Aubiere Cedex, France
²⁹Department of Physics, Lund University, Box 118, SE-221 00 Lund, Sweden
³⁰Institut für Kernphysik, University of Muenster, D-48149 Muenster, Germany
³¹Myongji University, Yongin, Kyonggido 449-728, Korea
³²Nagasaki Institute of Applied Science, Nagasaki-shi, Nagasaki 851-0193, Japan
³³University of New Mexico, Albuquerque, New Mexico 87131, USA
³⁴New Mexico State University, Las Cruces, New Mexico 88003, USA
³⁵Oak Ridge National Laboratory, Oak Ridge, Tennessee 37831, USA
³⁶IPN-Orsay, Université Paris Sud, CNRS-IN2P3, BP1, F-91406 Orsay, France
³⁷PNPI, Petersburg Nuclear Physics Institute, Gatchina, Russia
³⁸RIKEN, The Institute of Physical and Chemical Research, Wako, Saitama 351-0198, Japan
³⁹RIKEN BNL Research Center, Brookhaven National Laboratory, Upton, New York 11973-5000, USA
⁴⁰Saint Petersburg State Polytechnic University, St. Petersburg, Russia
⁴¹Instituto de Física, Universidade de São Paulo, Caixa Postal 66318, São Paulo CEP05315-970, Brazil
⁴²System Electronics Laboratory, Seoul National University, Seoul, South Korea
⁴³Chemistry Department, Stony Brook University, SUNY, Stony Brook, New York 11794-3400, USA
⁴⁴Department of Physics and Astronomy, Stony Brook University, SUNY, Stony Brook, New York 11794, USA
⁴⁵SUBATECH (Ecole des Mines de Nantes, CNRS-IN2P3, Université de Nantes), BP 20722-44307, Nantes, France
⁴⁶University of Tennessee, Knoxville, Tennessee 37996, USA
⁴⁷Department of Physics, Tokyo Institute of Technology, Tokyo 152-8551, Japan
⁴⁸Institute of Physics, University of Tsukuba, Tsukuba, Ibaraki 305, Japan
⁴⁹Vanderbilt University, Nashville, Tennessee 37235, USA
⁵⁰Advanced Research Institute for Science and Engineering, Waseda University,
17 Kikui-cho, Shinjuku-ku, Tokyo 162-0044, Japan
⁵¹Weizmann Institute, Rehovot 76100, Israel
⁵²Yonsei University, IPAP, Seoul 120-749, Korea

(Received 1 July 2005; published 2 August 2006)

Azimuthal correlations of jet-induced high- p_T charged hadron pairs are studied at midrapidity in Au + Au collisions at $\sqrt{s_{NN}} = 200$ GeV. The distribution of jet-associated partner hadrons ($1.0 < p_T < 2.5$ GeV/c) per trigger hadron ($2.5 < p_T < 4.0$ GeV/c) is found to vary with collision centrality, in both shape and yield, indicating a significant effect of the nuclear collision medium on the jet fragmentation process.

Energetic collisions between heavy ions at the Relativistic Heavy Ion Collider (RHIC) have been shown to produce matter with extremely high energy density [1]. This matter has been observed to strongly suppress the yield of hadrons with large transverse momenta in central Au + Au collisions, compared to yields in $p + p$ collisions scaled by the number of binary nucleon-nucleon collisions [2–5]. Such a suppression was predicted to result from energy loss of hard-scattered partons (light quarks and gluons) traversing the dense matter prior to forming the observed hadrons [6,7]. If the parton encounters a sufficient amount of dense matter, the energy loss could strongly modify its fragmentation into jets of hadrons.

Strong suppression of the awayside jet has been observed at RHIC [8]. However, it is unclear at present how the lost energy is transported by the dense medium, and how the parton-medium interaction affects the fragmentation process. Recently, there have been predictions that the coupling of jets to a strongly interacting medium may modify the angular distribution and number of jet fragments [9–16]. Quarks from hard scattering processes may recombine with thermal quarks from the dense medium [9,10]. Comoving radiated gluons may produce a “wake” in the medium, further increasing the number of quarks available for building hadrons in the jet fragmentation process [11,13]. It has even been proposed that the energy deposited in the medium creates a shock wave around the propagating parton, thereby creating a “conical flow” akin to a sonic boom in a fluid [14–16]. To investigate the transport of lost parton energy, the PHENIX experiment at RHIC measures azimuthally correlated hadrons arising from jet fragmentation as a function of centrality in Au + Au collisions. Such studies, in effect, use hard-scattered partons as short-wavelength probes of the produced medium.

The analysis presented in this Letter uses data from $\sqrt{s_{NN}} = 200$ GeV Au + Au collisions in the PHENIX 2002 data set. Charged particles are reconstructed in the central arms of PHENIX using drift chambers, each with azimuthal coverage of $\pi/2$, and two layers of multiwire proportional chambers with pad readout (PC1, PC3) [17]. Pattern recognition is based on a combinatorial Hough transform in the track bend plane, with the polar angle determined by PC1 and the collision vertex along the beam direction [18]. Particle momenta are measured with a resolution $\delta p/p = 0.7\% \oplus 1.0\% p$ (GeV/ c). To reject most background from albedo, conversions, and decays, a confirmation hit is required within a 2σ matching window in PC3 [2]. The Au + Au event centrality is determined using the PHENIX beam-beam counters (BBC) and zero-degree calorimeters [19].

The traditional identification of jets through hadronic calorimetry and cluster algorithms is problematic in Au + Au collisions at RHIC, since low-energy jets

(<10–20 GeV) are overwhelmed by other produced particles in the underlying event and high-energy jets are relatively rare at $\sqrt{s_{NN}} = 200$ GeV. Instead, we study hard-scattered single partons and parton pairs through angular correlations of high- p_T hadron pairs. We examine the distribution of pairs over relative azimuthal angle $dN^{AB}/d(\Delta\phi)$, where A and B denote charged particles in the PHENIX pseudorapidity acceptance ($|\eta| < 0.35$) and in p_T bins $2.5 \text{ GeV}/c < p_T^A < 4.0 \text{ GeV}/c$ (“trigger”) and $1.0 \text{ GeV}/c < p_T^B < 2.5 \text{ GeV}/c$ (“partner”). Pairs from fragments of the same jet are expected to appear near $\Delta\phi \sim 0$, while $\Delta\phi \sim \pi$ indicates one hadron each from the outgoing hard-scattered parton pair (hereafter “dijet”).

The PHENIX acceptance at central rapidity is nonuniform in azimuth. We correct for the shape of the acceptance in $\Delta\phi$ through the standard approach of constructing a correlation function, area normalized, utilizing pairs from mixed events:

$$C(\Delta\phi) \equiv \frac{Y_{\text{same}}^{AB}(\Delta\phi) \int Y_{\text{mixed}}^{AB}(\Delta\phi) d(\Delta\phi)}{Y_{\text{mixed}}^{AB}(\Delta\phi) \int Y_{\text{same}}^{AB}(\Delta\phi) d(\Delta\phi)} \propto \frac{dN^{AB}}{d(\Delta\phi)}, \quad (1)$$

where $Y_{\text{same}}^{AB}(\Delta\phi)$ and $Y_{\text{mixed}}^{AB}(\Delta\phi)$ are, respectively, the uncorrected yields of pairs in the same event and in mixed events, each of which are chosen uniformly within each data sample.

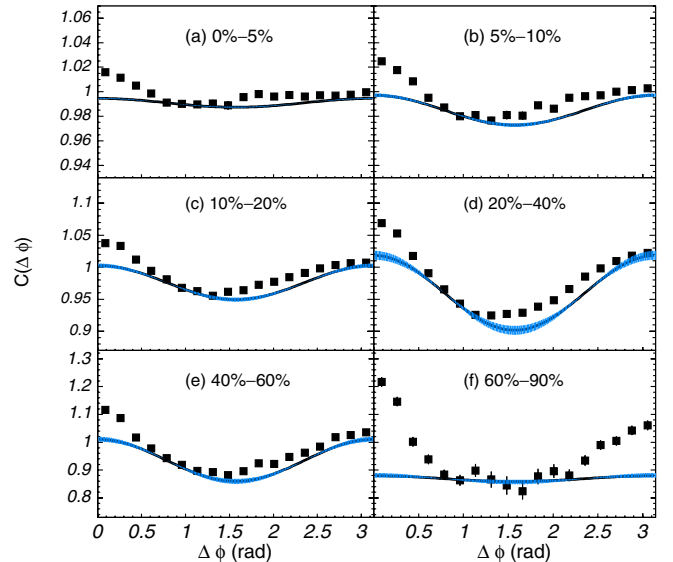


FIG. 1 (color online). Correlation functions, $C(\Delta\phi)$, for pairs of charged hadrons with $2.5 \text{ GeV}/c < p_T^A < 4.0 \text{ GeV}/c$ and $1.0 \text{ GeV}/c < p_T^B < 2.5 \text{ GeV}/c$ in different bins of collision centrality from the most central (a) 0%–5% to the most peripheral (f) 60%–90%. The solid bands indicate the estimate of the background pair component (see text) within one unit of its systematic error.

The correlation functions are shown in Fig. 1, folded into the range $0 < \Delta\phi < \pi$. For the most peripheral collisions [cf. Fig. 1(f)], the correlation function shows two well-defined peaks centered at $\Delta\phi = 0$ and $\Delta\phi = \pi$, which we can attribute to (di)jet pairs. For more central collisions, there is a similar peak at $\Delta\phi = 0$, a broader peak at $\Delta\phi = \pi$, and the apparent minima appear at $\Delta\phi < \pi/2$. These features reflect a mixture of (di)jet pairs and underlying events with particle flow along the reaction plane [20].

In order to extract and examine the jet-induced pairs, we analyze the pair distribution in the context of a *two-source model*, assuming that each hadron can be attributed to either (i) a jet fragmentation source or (ii) the underlying event. Additionally, we assume that the ϕ distributions for A or B inclusive single particles, summed over both sources, have a shape proportional to $\{1 + 2\langle v_2^A \text{ or } B \rangle \times \cos[2(\phi - \Phi_{RP})]\}$ relative to azimuthal angle Φ_{RP} of the reaction plane of each event. All pairs which are not from the same jet or dijet fragmentation are termed *background pairs*, and are taken to have no angular correlation beyond having their distributions respect the same reaction plane. In principle, contributions from resonance decays and global transverse momentum conservation can also affect the distribution of background pairs, but we estimate these effects to be negligible for these p_T ranges and the PHENIX η acceptance. The distribution of background pairs over $\Delta\phi$ is then proportional to $[1 + 2\langle v_2^A v_2^B \rangle \times \cos(2\Delta\phi)]$ [20].

Given a normalization, $C(\Delta\phi)$ can then be decomposed into two pieces, one proportional to the distribution of background pairs and another $J(\Delta\phi)$ proportional to that of the (di)jet pairs:

$$C(\Delta\phi) = b_0[1 + 2\langle v_2^A v_2^B \rangle \cos(2\Delta\phi)] + J(\Delta\phi). \quad (2)$$

We approximate $\langle v_2^A v_2^B \rangle = \langle v_2^A \rangle \langle v_2^B \rangle$, and we measure $\langle v_2^A \rangle$ and $\langle v_2^B \rangle$ for each centrality and particle p_T bin through a standard reaction-plane analysis using the PHENIX BBC to reconstruct the reaction plane event by event. The large rapidity gap, $\Delta\eta > 2.75$, between the central arm acceptance and the BBC acceptance substantially reduces non-flow contributions to the measured v_2 values, particularly those arising from (di)jets. The results are shown in Table I; they are consistent with prior PHENIX v_2 measurements [21], where available.

The average level of the background b_0 can, in principle, be fixed by making an assumption about the shape of the (di)jet-pair distribution. However, since we wish to measure the shape of the (di)jet azimuthal correlations, we use a technique that requires no such *a priori* assumptions. The simplest assumption allowing b_0 to be fixed is that $dN_{(di)jet}^{AB}/d(\Delta\phi)$ is zero for at least one value of $\Delta\phi$ (i.e., $\Delta\phi_{\min}$). We refer to this as the ZYAM (“zero yield at minimum”) assumption for the (di)jet-pair distribution. The ZYAM condition is met by varying b_0 until the back-

TABLE I. Anisotropy values for bins A ($2.5 < p_T < 4.0$ GeV/ c) and B ($1.0 < p_T < 2.5$ GeV/ c), shown with statistical errors, and values of ϕ_{\min} (see text). The relative systematic errors on the anisotropies are estimated to be $\pm 6\%$ for the five most central samples and $\pm 40\%$ for the most peripheral sample. The systematic errors on the v_2 's are dominated by the uncertainty in the correction for reaction plane resolution [21], and we assume them to be completely correlated between the two p_T bins in each centrality sample.

Centrality (%)	$\langle v_2^B \rangle$	$\langle v_2^A \rangle$	ϕ_{\min} (rad)
0–5	0.035 ± 0.001	0.052 ± 0.007	0.94
5–10	0.062 ± 0.001	0.100 ± 0.005	0.96
10–20	0.095 ± 0.0005	0.144 ± 0.003	0.98
20–40	0.146 ± 0.0004	0.208 ± 0.003	0.91
40–60	0.171 ± 0.001	0.236 ± 0.006	0.86
60–90	0.066 ± 0.001	0.091 ± 0.004	1.06

ground component matches a functional fit to the correlation function at one point $\Delta\phi_{\min}$, as illustrated by the solid bands in Fig. 1. The systematic error on b_0 associated with this procedure (see Fig. 2) was estimated by using a variety of functional forms that matched the data.

A nonzero yield of (di)jet pairs at $\Delta\phi_{\min}$ would invalidate the ZYAM assumption and result in an overestimate of the value of b_0 . To verify that we are not making a significant error in the normalization of the background, we have independently estimated the b_0 values using the AB pair combinatorial rate, corrected for a slight bias

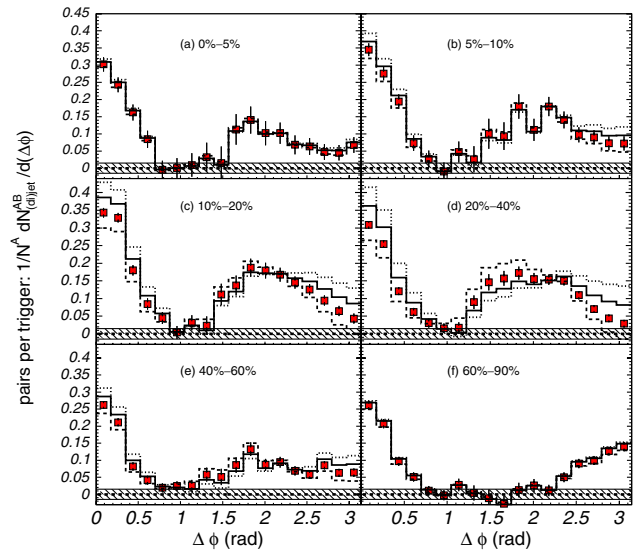


FIG. 2 (color online). Jet-pair distributions $dN_{(di)jet}^{AB}/d(\Delta\phi)$ for different centralities, normalized per trigger particle. The shaded bands indicate the systematic error associated with the determination of $\Delta\phi_{\min}$. The dashed (solid) curves are the distributions that would result from increasing (decreasing) $\langle v_2^A v_2^B \rangle$ by one unit of the systematic error; the dotted curve would result from decreasing by two units.

introduced by mixing events of different multiplicity within the same centrality class [22]. These independent estimates are consistent with the ZYAM-determined values for b_0 , confirming that we are not significantly overestimating the background levels.

Once $\langle v_2^A v_2^B \rangle$ and b_0 are fixed, we can extract $J(\Delta\phi)$ and the fully corrected (di)jet pairs distribution $dN_{(\text{di})\text{jet}}^{AB}/d(\Delta\phi)$. We construct the conditional yield distribution of jet-associated partners per trigger:

$$\frac{1}{N^A} \frac{dN_{(\text{di})\text{jet}}^{AB}}{d(\Delta\phi)} = \frac{J(\Delta\phi)}{\int C(\Delta\phi')d(\Delta\phi')} \frac{N^{AB}}{N^A}. \quad (3)$$

Here, N^A is the number of triggers and N^{AB} is the total number of AB pairs in the event sample. Assuming that the pair efficiency is the product of the single particle efficiencies, the trigger (A) efficiency cancels in Eq. (3). Thus, the ratio is corrected for acceptance and reconstruction efficiency [5] of the lower- p_T B particles; the systematic error on this correction leads to a 10% uncertainty on the associated yields.

The conditional yields of (di)jet-induced partners per trigger are shown in Fig. 2. For the most peripheral event sample the (di)jet-associated yield distribution has an appearance we might expect from a normal (di)jet fragmentation process [23]: a well-defined nearside peak around $\Delta\phi = 0$ and a somewhat wider awayside peak around $\Delta\phi = \pi$. For more central event samples the shape of the nearside peak is essentially unchanged while the associated yield in the nearside peak increases, indicating some change in the fragmentation process.

The much more dramatic change, however, is in the awayside peak, which is considerably broader in all the event samples more central than 60%. In midcentral and central collisions there is a local minimum at $\Delta\phi = \pi$. The existence of these local minima *per se* is not significant once we take the systematic errors on $\langle v_2^A v_2^B \rangle$ into account (see below), but it is clear that the awayside peaks in all the more central samples have a very different shape than in the most peripheral sample.

Given the dramatic results for the awayside peaks seen in Fig. 2, it is important to establish that they are not simply artifacts created by our method for background pair subtraction. If we relax the ZYAM assumption and lower b_0 slightly, the effect on any (di)jet-pair distribution would essentially be to raise it by a constant, which would not change the presence of the local minima at $\Delta\phi = \pi$, but would increase the per trigger yields. ZYAM derived yields are lower limit yields [20].

Changes to our estimate for $\langle v_2^A v_2^B \rangle$ can alter the shape of the (di)jet distribution for some centrality samples, but the result of awayside broadening with centrality remains robust. The curves in Fig. 2 show the distributions that would result if the $\langle v_2^A v_2^B \rangle$ products were arbitrarily lowered by one and two units of their systematic error. With a

two-unit shift the shape in the midcentral would no longer show significant local minima at $\Delta\phi = \pi$. However, the widths of the awayside peaks are clearly still much greater than in the peripheral sample and the distributions in the two most central samples are hardly changed at all in shape. Even lower values of $\langle v_2^A v_2^B \rangle$ could be contemplated, but they would still not change the qualitative result of awayside broadening. And, such low $\langle v_2^A v_2^B \rangle$ values would also require a severe breakdown of the assumption $\langle v_2^A v_2^B \rangle = \langle v_2^A \rangle \langle v_2^B \rangle$, indicating that these background pairs have a large, hitherto-unknown source of azimuthal anticorrelation.

Convoluting the jet fragments' angles with respect to their parent partons and the acoplanarity between the two partons [23] would yield a Gaussian-like shape in $\Delta\phi$, possibly broadened through jet quenching [13,24]. The observed shapes in the awayside peaks cannot result from such a convolution.

We define the part of the $\Delta\phi$ distribution in $|\Delta\phi| < \Delta\phi_{\text{min}}$ as the ‘‘nearside’’ peak and $|\Delta\phi| > \Delta\phi_{\text{min}}$ as the ‘‘awayside’’ peak. Each peak is characterized by its yield of associated partners per trigger and by its rms width. We measure these for the full peak in the distribution over all values of $\Delta\phi$; the folded distributions over $0 < \Delta\phi < \pi$ shown here contain only half of each full peak's shape. These yields and widths are plotted in Fig. 3 for the different Au + Au centrality samples, along with the same quantities for 0%–20% central $d + \text{Au}$ collisions at $\sqrt{s_{NN}} = 200$ GeV [23]. The yields and widths for the near- and awayside peaks in peripheral Au + Au collisions are consistent with those in $d + \text{Au}$ collisions. The yields of both the near- and awayside peaks increase from peripheral to midcentral collisions, and then decrease for the most central collisions. The nearside width is unchanged with centrality, while the awayside width in-

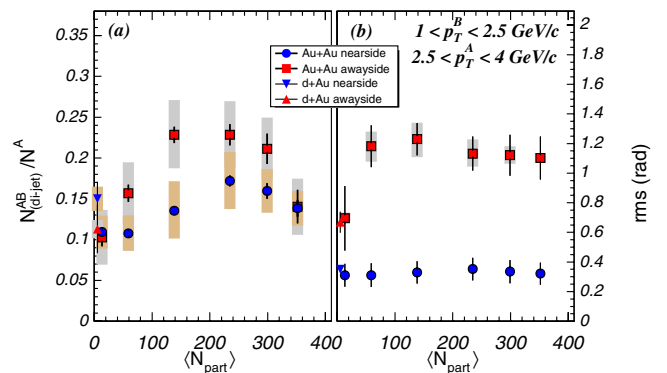


FIG. 3 (color online). (a) Associated yields for near- and awayside peaks in the jet-pair distribution, and (b) widths (rms) of the peaks in the full $0-2\pi$ distributions; plotted versus the mean number of participating nucleons for each event sample. Triangles show results from 0%–20% central $d + \text{Au}$ collisions at the same $\sqrt{s_{NN}}$ [23]. Bars show statistical errors, shaded bands systematic.

creases substantially from the 60%–90% sample to the 40%–60% sample, and then remains constant with centrality.

In summary, we have presented correlations of high momentum charged hadron pairs as a function of collision centrality in Au + Au collisions. Utilizing a novel technique, we extract the jet-induced hadron pair distributions and show that the dense medium formed in Au + Au collisions at RHIC modifies jet fragmentation. In central and midcentral collisions the awayside angular distribution is significantly broadened relative to peripheral and $d + Au$ collisions, and appears to be non-Gaussian. The shapes of the awayside $\Delta\phi$ distributions for non-peripheral collisions are apparently not consistent with Gaussian broadening of the peripheral Au + Au awayside. However, the broadening and possible changes in shape of the awayside jet are suggestive of recent theoretical predictions of dense-medium effects on fragment distributions [14–16,25]. The broadened shapes of the awayside distributions also imply that integration of the awayside peak in a narrow angular range around $\Delta\phi = \pi$ yields fewer associated partners in central collisions than in peripheral or $d + Au$ collisions, as seen elsewhere [8,22]; but integrating over the entire broadened peak recovers the jet partners in the range $1.0 \text{ GeV}/c < p_T^B < 2.5 \text{ GeV}/c$ used here. Even though two-particle correlations do not allow for full reconstruction of the jet fragmentation function, these data provide an entirely new way to probe the hot, dense medium formed in heavy ion collisions.

We thank the staff of the Collider-Accelerator and Physics Departments at BNL for their vital contributions. We acknowledge support from the Department of Energy and NSF (USA), MEXT and JSPS (Japan), CNPq and FAPESP (Brazil), NSFC (China), CNRS-IN2P3 and CEA (France), BMBF, DAAD, and AvH (Germany), OTKA (Hungary), DAE and DST (India), ISF (Israel), KRF and CHEP (Korea), RMIST, RAS, and RMAE (Russia), VR and KAW (Sweden), U.S. CRDF for the

FSU, U.S.-Hungarian NSF-OTKA-MTA, and U.S.-Israel BSF.

*Deceased.

†PHENIX spokesperson.

Electronic address: zajc@nevis.columbia.edu

- [1] K. Adcox *et al.*, Nucl. Phys. **A757**, 184 (2005).
- [2] K. Adcox *et al.*, Phys. Rev. Lett. **88**, 022301 (2001).
- [3] S. S. Adler *et al.*, Phys. Rev. Lett. **91**, 072301 (2003).
- [4] J. Adams *et al.*, Phys. Rev. Lett. **91**, 172302 (2003).
- [5] S. S. Adler *et al.*, Phys. Rev. C **69**, 034910 (2004).
- [6] J. D. Bjorken, Fermilab Report No. FERMILAB-PUB-82-059-THY, 1982.
- [7] X. N. Wang and M. Gyulassy, Phys. Rev. Lett. **68**, 1480 (1992); X. N. Wang, Phys. Rev. C **58**, 2321 (1998).
- [8] C. Adler *et al.*, Phys. Rev. Lett. **90**, 032301 (2003); **90**, 082302 (2003).
- [9] V. Greco *et al.*, Phys. Rev. Lett. **90**, 202302 (2003); Phys. Rev. C **68**, 034904 (2003).
- [10] R. C. Hwa and C. B. Yang, Phys. Rev. C **70**, 024905 (2004); J. Phys. G **30**, S1117 (2004).
- [11] R. Fries *et al.*, Phys. Rev. Lett. **94**, 122301 (2005).
- [12] A. Majumder, E. Wang, and X. N. Wang, nucl-th/0412061.
- [13] N. Armesto, C. Salgado, and U. A. Wiedemann, Phys. Rev. Lett. **93**, 242301 (2004).
- [14] J. Casalderrey-Solana, E. V. Shuryak, and D. Teaney, J. Phys.: Conf. Ser. **27**, 22 (2005).
- [15] H. Stöcker, Nucl. Phys. **A750**, 121 (2005).
- [16] J. Ruppert and B. Muller, Phys. Lett. B **618**, 123 (2005).
- [17] K. Adcox *et al.*, Nucl. Instrum. Methods Phys. Res., Sect. A **499**, 469 (2003).
- [18] J. Mitchell *et al.*, Nucl. Instrum. Methods Phys. Res., Sect. A **482**, 491 (2002).
- [19] K. Adcox *et al.*, Phys. Rev. C **69**, 024904 (2004).
- [20] N. N. Ajitanand *et al.*, Phys. Rev. C **72**, 011902 (2005).
- [21] S. S. Adler *et al.*, Phys. Rev. Lett. **91**, 182301 (2003).
- [22] S. S. Adler *et al.*, Phys. Rev. C **71**, 051902 (2005).
- [23] S. S. Adler *et al.*, Phys. Rev. C **73**, 054903 (2006).
- [24] J.-W. Qiu and I. Vitev, hep-ph/0410218.
- [25] N. Armesto *et al.*, Phys. Rev. C **72**, 064910 (2005).